A General Approach for Deformation Induced Stress on Flexible Electronics

Heetaek Lim
Silvaco Inc.
North Chelmsford, MA
heetaek.lim@silvaco.com

Sungwon Kong
Silvaco Inc.
Santa Clara, CA
sungwon.kong@silvaco.com

Eric Guichard
Silvaco Inc.
Santa Clara, CA
eric.guichard@silvaco.com

Andreas Hoessinger
Silvaco Europe Ltd.
Cambridge, United Kingdom
andreas.hoessinger@silvaco.com

***Abstract*—We present a simulation approach that is based on non-linear finite element method. This simulation flow allows to calculate large deformation field and associated stress and strain. The obtained simulation result agrees well with analytic solution. We extend this simulation method to evaluate the impacts of the deformation induced stress on device performance as well as structural integrity.**

Keywords—flexible devices, deformation, bending stress, strain

I. INTRODUCTION

Flexible electronics that can bend are attracting wider attention from both academia and industry. In those devices, the bending induced effects can bring significant deviation from their designed values and may influence their effective use in the target application. Therefore, it is critical to understand the behavior of devices and circuits under different bending conditions. A few articles have reported stress induced effects, but most of their modeling approaches are based on somewhat simplistic analytical models, which are only valid for small deformations [1-3]. Not much has been reported in the literature about the analytical models that capture the nonlinear relationship between loading force and maximum stress.

The objective of this work is to develop the capacity to simulate and predict the device response under various bending conditions, which can undergo beyond linear deformation regions. This capacity enables us to predict how numerous parameters such as the crystal structure of the electronic substrate, the design of devices and circuits and their layout with respect to various crystal axes, and the energy band structure are affected by deformation induced stress and strain through variations in electrical parameters.

II. SIMULATION METHOD

A. Prescribed Boundary Conditions

Flexible devices can experience different types of deformations such as tensile, compressive, shearing, bending, and torsional. As a general approach to deal with any combination of those deformation modes, we apply prescribed motions at boundaries.

To this end, we create rigid surfaces at boundaries such that motion of nodal points at the rigid surface follows rigid body kinematics:

$$x_i = x_{ref} + R(\theta_{ref})(X_i - X_{ref}) \tag{1}$$

where x_{ref} (reference point translation) and θ_{ref} (reference point rotation) are simulation variables, and R is 3×3 rotation matrix for the given rotation angle.

The problem of imposing kinematic constraints at the boundaries lead to numerical schemes to solve constrained systems.

B. Numerical Treatment of Constraints

For the discussion that follows, we consider the following linear system of algebraic equations resulting from the regular finite element discretization [4]

$$Kd = f \tag{2}$$

where d is the unknown displacement vector, f is the given force vector, and K is symmetric positive definite stiffness matrix.

The problem (2) can be obtained as the stationary point of the following potential

$$\Pi(d) = \frac{1}{2}d^T K d - d^T f \tag{3}$$

Our goal is to find d that is the stationary point of $\Pi(d)$ and satisfies the additional linear constraint

$$c(d) = Q^T d - \bar{d}_c \tag{4}$$

where $\bar{d}_c$ accounts for the prescribed boundary condition derived from Eq. (1).

C. The Penalty Method

Define the penalty functional

$$\Pi_\kappa(d) = \Pi(d) + \frac{1}{2}\kappa c(d)^2 \tag{5}$$

for a penalty parameter $\kappa > 0$.

We find d_κ that is the stationary point of $\Pi_\kappa(d)$ by taking the first variation

$$\frac{\partial \Pi_\kappa}{\partial d} = K d_\kappa - f + \kappa c(d_\kappa) Q = 0 \tag{6}$$

We obtain

$$[K + \kappa Q Q^T] d_\kappa = f + \kappa \bar{d}_c Q \tag{7}$$

The final system consists of the symmetric and positive definite stiffness matrix and a single unknown filed, which is equivalent to the original system given by Eq. (2).

The key to the success of the method is the choice of the penalty parameter. A small parameter will impose the constraint loosely. The higher parameter makes the system more ill-conditioned, hence introduce more round-off error. Thus the parameter has to be determined in a manner that minimizes the sum of round-off error and approximation error. According to [5], the optimal parameter in double precision arithmetic is given by

$$\kappa_{opt} = 10^8 K_{min} \tag{8}$$

where K_{min} denotes the smallest diagonal component in **K**.

III. LARGE DEFORMATION FORMULATION

A. Deformation Gradient

Once the displacement filed is determined by solving the aforementioned constrained problem, we can calculate stress and strain from the displacements as shown in [6].

For the simplest shape finite element composed of a 3-node triangular form with displacement parameters at each vertex (a 9-degree of freedom element), a linear triangle initial positions in the element may be specified using standard interpolation as

$$X = b_1X_1 + b_2X_2 + b_3X_3 \tag{9}$$

similarly, for the current configuration in lower case by x:

$$x = b_1x_1 + b_2x_2 + b_3x_3 \tag{10}$$

If necessary, the displacement vector may be deduced as

$$u = b_1u_1 + b_2u_2 + b_3u_3 \tag{11}$$

Furthermore, the natural (area) coordinates satisfy the constraint $b_1 + b_2 + b_3 = 1$.So, we can alternatively write the initial configuration as

$$X = X_3 + \begin{bmatrix} (X_1 - X_3)_x & (X_2 - X_3)_x \\ (X_1 - X_3)_y & (X_2 - X_3)_y \end{bmatrix} \begin{pmatrix} b_1 \\ b_2 \end{pmatrix} \tag{12}$$

Thus we construct the Jacobian transformation for the reference frame, which we call **J**, that contains vectors along the edges of the triangle as its columns and this matrix describes the mapping from natural coordinates to material coordinates. If we wish to go the other way, we will need to invert this matrix such that

$$\begin{pmatrix} b_1 \\ b_2 \end{pmatrix} = J^{-1}(X - X_3) \tag{13}$$

Similarly, for the current frame

$$x = x_3 + j\begin{pmatrix} b_1 \\ b_2 \end{pmatrix} \tag{14}$$

where **j** is a matrix made up of vectors along the edges of the triangle in current coordinates. Now we can define the entire mapping as

$$x(X) = x_3 + jJ^{-1}(X - X_3) \tag{15}$$

Taking the derivative of this function with respect to **X,** the deformation gradient is given by

$$F = \frac{\partial x}{\partial X} = jJ^{-1} \tag{16}$$

B. Deformation Induced Stress/Strain

In the present work we assume that a simple St.Venant-Kirchhoff material model may be used to express the stresses from the deformations. The second Piola-Kirchhoff stresses are thus given by

$$S = DE \tag{17}$$

where **D** are constant elastic moduli and the Green-Lagrange strains **E** are given in terms of the deformation tensor as

$$E = \frac{1}{2}(FF^T - I) \tag{18}$$

Suppose we write our deformation gradient as

$$\frac{\partial x}{\partial X} = \frac{\partial (X+u)}{\partial X} = I + H \tag{19}$$

That is the deformation gradient is the identity (no deformation) plus some amount of deformation. Now we can rewrite the Green-Lagrange strain as

$$\begin{aligned} E &= \frac{1}{2}[(I + H)^T(I + H) - I] \\ &= \frac{1}{2}(H^T + H) + \frac{1}{2}H^TH \end{aligned} \tag{20}$$

This indicates that the Green-Lagrange strain is infinitesimal strain plus quadratic term, which makes the strain finite and nonlinear. The linear infinitesimal strain is a good approximate for small deformations. Unfortunately, it is not invariant to rotations, which leads to artifacts if it is used for large deformations such as bending simulation.

We can see from the definition of traction that stress maps normals to forces. Therefore it is important to distinguish where these normals and forces are defined. Both normals and forces are defined in the reference (undeformed) frame for the second Piola-Kirchhoff stress. However, a Cauchy stress, where both normals and forces are in the current (deformed) frame, is often used in engineering practices. Thus the following transformation can be used to get the Cauchy stresses

$$\sigma = \frac{1}{det(F)}FSF^T \tag{21}$$

A conjugate strain to the Cauchy stress in large deformations is Almansi strain, which defined as

$$e = \frac{1}{2}(I - F^{-T}F^{-1}) \tag{22}$$

In terms of the displacement field, it is written as

$$e = \frac{1}{2}\left(\frac{\partial u^T}{\partial x} + \frac{\partial u}{\partial x} - \frac{\partial u^T}{\partial x}\frac{\partial u}{\partial x}\right) \tag{23}$$

The key here is that the derivatives are with respect to the deformed positions, **x**.

IV. VERIFICATION

For a cantilevered straight beam subjected to a free end moment (Fig. 1), the analytic solution can be obtained as in [7]

$$\theta_x = \frac{\mathrm{ML}}{\mathrm{EI}} \tag{24}$$

$$u_z = \mathrm{L} - \frac{L}{\theta}\sin\theta \tag{25}$$

$$u_y = \frac{L}{\theta}\tan\frac{\theta}{2}\sin\theta \quad (26)$$

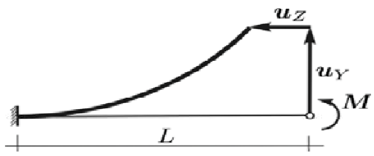

Fig. 1. Pure bending of a cantilever beam

With beam depth h, the maximum fiber stress at the fixed end can be also obtained as

$$\sigma = \frac{\mathrm{Mh}}{2I} = \frac{\mathrm{Eh}}{2L}\theta_x \quad (27)$$

If we apply prescribed boundary rotations given by Eq. (24) on left and right ends of a simple beam with length 2L, we can expect that the bending deformation is nearly constant along the beam. As a result, the deflection and maximum fiber stress of the beam center should be given by Eq. (26) and Eq. (27) respectively. The selected properties of the simple beam are: L=10, h=2, I=0.67, and E=10^{10}.

Fig. 2 shows simulation results with deformed mesh and stress/strain contour for 50 degree rotations. It is worthwhile to mention that the mesh is so nicely deformed that we do not need any re-meshing during the large deformation analysis.

TABLE I presents comparisons between the analytic solution and that obtained with FE simulations for various end rotation angles, and no significant discrepancies are found.

a) deformed mesh

b) Cauchy stress (XX component)

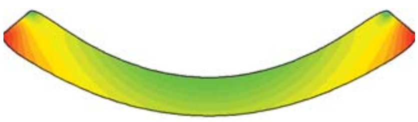

c) Almansi strain (XX component)

Fig. 2. Bending of a simple beam (50 degree end rotations)

TABLE I. BEAM DEFLECTION AND FIBER STRESS

Angle (degree)	Deflection			Stress (1e09)		
	Exact	Sim.	Error %	Exact	Sim.	Error %
10	0.87045	0.86824	0.25	1.74533	1.66168	4.79
20	1.72768	1.71010	1.01	3.49066	3.35006	4.02
30	2.55873	2.50000	2.29	5.23599	5.00583	4.39
40	3.35117	3.21394	3.21	6.98132	6.56258	5.99
50	4.09335	3.83022	6.42	8.72655	7.96053	8.77

V. APPLICATION

A. TFT Bending Simulation

The newly-developed method is used to accurately model a-IGZO TFT on a flexible substrate in order to determine structural integrity, performance and reliability, as well as predicting structural failures. The target model is composed of six different material regions including IGZO/Cr (gate metal)/PI stack. Since the critical point in thin film usually happens to be the most brittle layer that fails to resist to applied bending stress, SiO2 buffer layer between film and PI substrate is introduced to resist such stress induced failure. The mechanical properties used for this simulation are listed in TABLE II.

TABLE II. SIMULATION INPUT

	Young's modulus (dyne/cm^2)	Poisson ratio	Thickness (um)
IGZO	1.37e12	0.36	0.2
Si3N4	2.5e12	0.23	0.3
Mo	3.3e12	0.38	0.2
Cr	2.79e12	0.21	0.2
SiO2	0.7e12	0.17	buffer
PI	0.29e12	0.34	10

Fig. 3 shows transfer curve of IGZO thin film transistor in compressive stress and in tensile stress case. The inset plot shows the electron carrier distribution in tensile stress at the front channel (IGZO/gate insulator interface) shorten the channel length, which results in increased drain current. Please note that the bending radius (or angle of moment) is exaggerated and thus the degree of drain current change in moderate condition would be small without change of material parameters such as band gap or mobility.

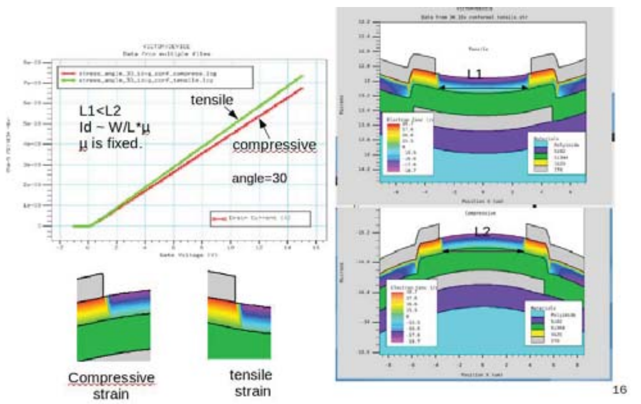

Fig 3. Transfer curve in compressive and tensile strain (top right is tensile and bottom right is compressive)

The following additional observations are obtained:

- Due to the cracks at the center of TFT. on-current is reduced and leakage current is increased.
- Buffer layers between film and PI substrate play an important role to prevent stress induced failure.
- Cracks are initiated around the edge of gate, source/drain overlap region and propagated over the whole TFT stack.

B. Device Simulation

Finally, the resulting deformed geometry and bending induced stress are passed over to subsequent device simulation to assess their impact on device performance. To this end, various end rotation angles (tensile and compressive) are applied and results are summarized in Fig. 4 and Fig 5.

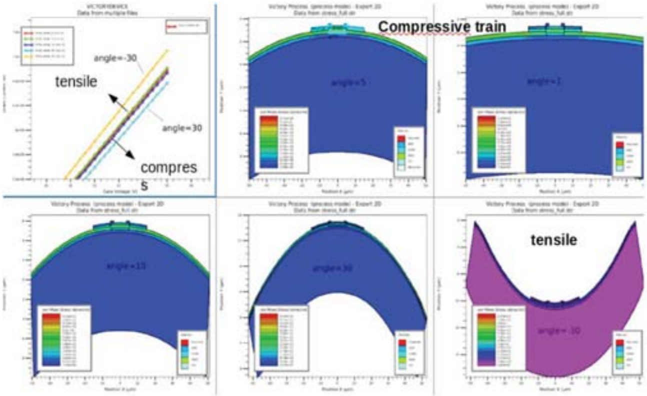

Fig. 4. Geometry and bending stress effects on the current

We can see that current with tensile strain is larger than compressive strain. We believe that this is related to reduced effective channel length shown by majority carrier. In a-IGZO material, tensile strain increases the inter-atomic distance among atoms. It reduces the energy level splitting between bonding and anti-bonding. The mobility increase for tensile strain can be correlated with a decrease in the electron-lattice interaction due to the decreased energy spacing in the direction parallel to the current flow. This decreases the effective mass of the charge carriers and affects their mobility.

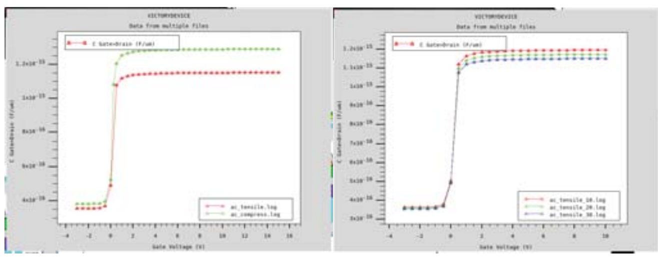

Fig.5 Bending effects on capacitance

VI. Conclusion

A geometric non-linear finite element approach has been developed to address ever increasing demand for simulation capacity to deal with deformation indued stress on flexible electronics. This is achieved by applying arbitrary motion at the boundaries including large rotations and translations, which makes this approach general without any limitations. The proposed capability has been implemented in the Victory Process simulation framework [8].

Comparisons between simulation result and analytic solution show an excellent agreements. We have also shown that this scheme can be used to model realistic problems with high accuracy, such as the optimization of TFT structure on a flexible substrate to determine substrate material and thickness that reduce the bending induced stress in brittle layers of the device. The device simulation will also help designers to understand the electrical behavior through simulated bending structure.

Given the fact that stress and strain accompanied by large deformation are usually determined by non-linear FEM calculations, we believe that this approach increases the predictive power in the design and evaluation steps.

References

[1] S. M. Lee, D. S. Shin, and I. Yun, "Degradation mechanisms of amorphous InGaZno thin-film transistors used in fordable displays by dynamic mechanical stress," IEEE Transactions on Electron Devices, vol. 64, No. 1, pp. 170-175, Jan. 2017.

[2] M. M. Billah, M. M. Hasan, and J. Jang, "Effect of tensile and compressive bending stress on electrical performance of flexible a-IGZO TFTs," IEEE Electron Device Letters, vol. 38, No. 7, pp. 890-893, July 2017.

[3] H. Heidari, N. Wacker, and R. Dahiya, "Bending induced electrical response variations in ultra-thin flexible chips and device modeling," Applied Physics Review, vol. 4, 2017.

[4] O. C. Zienkiewic and R. L. Taylor, "The finite element methods for solid and structural mechanics," Oxford, 2005.

[5] J.A. Landers and R.L. Taylor, "An augmented Lagrangian formulation for the finite element solution of the contact problems," Technical Report, UCB/SESM 85/09, University California at Berkeley, 1985.

[6] R.L. Taylor, Eugenio Onate, and Pere-Andreu Ubach, "Finite element analysis of membrane structures," Textile Composites and Inflatable Structures, pp. 47-68, Springer, 2005.

[7] J. C. Simo and L. Vu-Quoc, "A three-dimensional finite strain rod model. Part II: computational aspects," Computer Methods in Applied Mechanics and Engineering, vol. 49, pp. 79-116, 1986.

[8] Victory Process User's Manual, Silvaco Inc., USA.